Published in final edited form as:
J Nucl Med. 2009 September ; 50(9): 1387–1390. doi:10.2967/jnumed.109.061838.

New Agents and Techniques for Imaging Prostate Cancer

Atif Zaheer, **Steve Y. Cho**, and **Martin G. Pomper**
Russell H. Morgan Department of Radiology and Radiological Science, Johns Hopkins Medical Institutions, Baltimore, Maryland

Abstract

The successful management of prostate cancer requires early detection, appropriate risk assessment, and optimum treatment. An unmet goal of prostate cancer imaging is to differentiate indolent from aggressive tumors, as treatment may vary for different grades of the disease. Different modalities have been tested to diagnose, stage, and monitor prostate cancer during therapy. This review briefly describes the key clinical issues in prostate cancer imaging and therapy and summarizes the various new imaging modalities and agents in use and on the horizon.

Keywords

molecular imaging; MRI; PET; SPECT; radiopharmaceutical

Prostate cancer (PCa) is the most common malignancy among men in the United States, with mortality superseded only by lung cancer, accounting for 10% of all cancer-related deaths in 2008 (1). PCa is currently characterized by its TNM stage, Gleason score, and prostate-specific antigen (PSA) serum level. PSA testing is the mainstay of detection and has reduced the rate of death from PCa. However, there remains growing concern regarding the potential risk of overdiagnosis and, consequently, overtreatment of potentially indolent disease. The rate of over-diagnosis of PCa, defined as diagnosis in men who would not have clinical symptoms during their lifetime, has been estimated to be as high as 50% (2). Urinary incontinence and erectile dysfunction are not uncommon after radical prostatectomy. Although PSA is a good marker for assessing response to therapy and detecting recurrence, PSA lacks the ability to differentiate low-grade from high-grade cancers. New biomarkers such as the recently described stage-dependent urinary marker sarcosine (3) may soon rival PSA for monitoring the presence and extent of disease.

Conventional imaging, which includes CT, MRI, and ultra-sound, is currently used to detect organ-confined or metastatic disease for staging and determining prognosis. However, there is substantial room for improvement in the use of imaging for determining tumor grade and for identifying minimal, metastatic disease. At a recent workshop, the National Cancer Institute proposed intervention for PCa at 4 different levels (4). The roles of imaging in initial diagnosis, staging, disease recurrence after treatment, and assessment of response to therapy were discussed. Also discussed were the multiple new molecular imaging agents that are being tested and can be incorporated into the current paradigm of diagnosis, treatment, and rapid detection of recurrent disease. We will address new approaches to imaging PCa in the context of these 4 levels of intervention.

For correspondence or reprints contact: Martin G. Pomper, Johns Hopkins Medical Institutions, 1550 Orleans St., 492 CRB II, Baltimore, MD 21231. mpomper@jhmi.edu.

INITIAL DIAGNOSIS

The current standard for diagnosis of PCa is sextant biopsy guided by transrectal ultrasound. PCa is the only malignancy for which the diagnosis is made from tissue obtained on a blind biopsy. That technique tends to underestimate the histologic grade. The heterogeneous nature and multifocality of the tumor renders a blind biopsy inadequate in assessing tumor grade. Up to 28% of clinically significant cancers have been reported to go undetected by the traditional sextant biopsy method (5). Imaging data, which are not susceptible to the sampling error that accompanies biopsy, can enhance biopsy by allowing for a more targeted approach.

T2-weighted MRI provides higher spatial and contrast resolution than does transrectal ultrasound and CT but lacks specificity (6). Magnetic resonance spectroscopy (MRS) provides a noninvasive method of detecting low-molecular-weight biomarkers within the cytosol and extracellular spaces of the prostate. MRS relies on the loss of a normal citrate peak from the peripheral zone and an increase in the choline peak, an indirect marker of cell death. The ratio of (choline 1 creatine)/citrate in PCa exceeds the mean ratio found in healthy prostate tissue. Pulsed field gradients are generally used for localization using volumes of interest and include point-resolved spectroscopy and stimulated echo acquisition mode, summarized in an excellent review by Mueller-Lisse and Scherr (7). Although the addition of MRS to MRI alone does not significantly improve the accuracy of PCa detection, together they are more accurate than biopsy in certain regions of the prostate, such as the apex (8). MRS combined with MRI may also supplement standard biopsy guided by endorectal ultrasound (9). Measurement of prostate tumor (choline 1 creatine)/citrate and tumor volume by MRS imaging correlates with Gleason score (10). In a small clinical trial, improved spatial and spectral resolution were achieved at 7 T, allowing for more sensitive detection of spermine, a metabolite having an inverse correlation with the presence of tumor cells (11).

Despite the limited ability of ultrasound to delineate cancer, ultrasound has the advantage of low cost, wide availability, and speed over MR image–guided interventions. A recent study demonstrated the feasibility of prostate biopsy guided by fusion of transrectal ultrasound and MRI, with the entire procedure, including fusion, requiring about 10 min (12). Furthermore, with an ultrasound 3-dimensional (3D) navigation system, such as that developed by Bax et al. (13), needle guidance can be used for sampling small lesions. Tests of the accuracy of biopsy needle guidance in agar prostate phantoms showed a mean error of 1.8 mm in the 3D location of the biopsy core, with less than 5% error in volume estimation. Addition of MRS data to this approach may improve detection of PCa by a method that can be used by urologists in their office.

Albers et al. (14) recently demonstrated promising results by quantifying differences in hyperpolarized ^{13}C-labeled pyruvate and its metabolites (lactate and alanine) between the various histologic grades of PCa using the transgenic adenocarcinoma of mouse prostate (TRAMP) model. It was previously difficult to observe lactate and alanine with in vivo MRS studies as lipids resonate near the frequencies of these metabolites. However, ^{13}C-labeled substrates have recently been polarized using dynamic nuclear polarization to obtain tens of thousands–fold enhancement of the ^{13}C-NMR signals for the substrate and its metabolites. The method allows 3D visualization of the distribution of lactate, pyruvate, and alanine throughout the prostate and surrounding anatomy, providing a noninvasive method to detect tumors and regional lymph node metastasis. A strong correlation between metabolite levels and the grade of the tumor has been demonstrated by this technique (Fig. 1). Accordingly, hyperpolarized ^{13}C-pyruvate imaging, if successful in humans, has the potential to predict indolent versus aggressive disease. A phase 1 clinical study will be under

way in PCa patients in the fall of 2009, and a commercial dynamic nuclear polarizer for human studies is expected to be available in 2010.

Methylcholine labeled with ^{11}C, or ^{11}C-choline, has been tested as a radiopharmaceutical for PET of PCa. ^{11}C-choline is integrated into phospholipids in the cell membrane of tumor cells and represents the rate of tumor cell replication. Testa et al. showed that for detection and localization of primary PCa, ^{11}C-choline PET/ CT was found to have lower sensitivity than 3D MRS alone or in conjunction with MRI (3D MRS, 81%; 3D MRS and MRI, 88%) (15). The specificity for detection and localization were, however, comparable with the 3 modalities. In a recent study, no significant correlation was detected between ^{11}C-choline maximum standardized uptake value and PSA levels, Gleason score, or pathologic stage (16). The short physical half-life of ^{11}C has led to the development of an ^{18}F-labeled analog of choline. Kwee et al. showed that ^{18}Ffluorocholine can localize dominant areas of malignancy but may miss smaller tumor foci, with the highest diagnostic accuracy at a standardized uptake value of 5.6 or more (sensitivity, 64%; specificity, 90%; accuracy, 72%) (17). In one small study, ^{11}C-acetate PET demonstrated marked uptake in primary PCa and proved more sensitive than ^{18}F-FDG PET (18). Concerning another metabolic agent, namely ^{11}C-acetate, a larger number of patients are needed to determine the ultimate clinical utility for primary lesions.

Initial experience with anti-1-amino-3-^{18}F-fluorocyclobutane-1-carboxylic acid (anti-^{18}F-FACBC), a synthetic L-leucine analog, in 15 patients with either newly diagnosed or suspected recurrent PCa has been encouraging (19). In newly diagnosed patients, anti-^{18}F-FACBC correctly identified tumor in 40 of 48 prostate region sextants, with 7 of 9 patients demonstrating pelvic nodal uptake concordant with the clinical follow-up. Anti-^{18}F-FACBC was positive in all 4 patients with proved recurrence (negative capromab pendetide [ProstaScint; EUSA Pharma] findings in 3 of these patients) and was instrumental in directing biopsy to prove neoplastic recurrence in one patient in whom lymph nodes were not obviously enlarged.

STAGING

The TNM system describes the extent of intra- and extra-glandular disease, spread to lymph nodes, and the presence of distant metastasis. Patients with organ-confined disease tend to do better than those with extraglandular disease. The approach of combining dynamic contrast-enhanced MRI with T2-weighted MRI at 1.5 T has a specificity of 95% for the detection of extracapsular disease, with a sensitivity of 86% (20).

Pelvic lymph node metastases are considered the strongest predictor of disease recurrence and progression, and the presence of metastases often means the difference between local and systemic therapy. Small metastases or micrometastases cannot be detected using conventional size criteria. The use of lymphotropic ultrasmall superparamagnetic particles of iron oxide (USPIO) as a contrast agent for MRI enables reliable detection of metastases in pelvic lymph nodes smaller than 0.5 cm in patients with PCa. USPIO particles are consumed by macrophages in normal lymph nodes resulting in a signal decrease on T2/T2*-weighted MRI sequences. The technique demonstrates extremely high sensitivity (96%) and specificity (99%) for lymph nodes measuring between 5 mm and 1 cm in diameter, with the sensitivity dropping to 41% for nodes less than 5 mm in diameter (21). However, node-by-node comparison between the pre- and post-USPIO images renders interpretation time consuming.

Diffusion-weighted imaging (DWI) is an MRI technique based on the detection of random movement of water molecules, which is theoretically lower in cancers because they have higher cellular density than does surrounding tissue. The apparent diffusion coefficient is the

main outcome parameter of a diffusion-weighted image and has been shown to be a significant predictor of both adverse repeated biopsy findings and time to radical treatment (22). There is a recent trend toward the use of 2 or more functional MRI sequences concurrently, especially since the advent of DWI, which is fast and does not require exogenous contrast material. Studies that combine DWI with T2-weighted, contrast-enhanced, and MRS techniques have shown promising results (23). DWI may also correlate with a higher Gleason score (24). Diffusion-weighted sequences are typically T2/T2*-sensitive and potentially allow combination of cellular information with USPIO uptake in the same examination. The combination of reduced diffusion together with a relatively unchanged T2/T2* after USPIO administration in malignant lymph nodes may enable better detection of intranodal metastases. Xu et al. (25) recently used diffusion tensor imaging—a technique closely allied to DWI—to obtain measurements of PCa in vivo in patients undergoing radical prostatectomy and, later, ex vivo in the corresponding prostatectomy specimens. The results suggested that the apparent diffusion coeffi-cient contrast parallels the T2-weighted contrast, with the apparent diffusion coefficient being more specific than T2-weighted contrast for PCa within the peripheral zone. Diffusion anisotropy, an outcome parameter provided by diffusion tensor imaging, provides a unique contrast that differentiates benign prostatic hypertrophy within stroma from PCa in the central gland, whereas its utility for PCa in the peripheral zone is limited.

DISEASE RECURRENCE AFTER TREATMENT

Biochemical recurrence occurs in 20%–40% of patients within 10 y of “definitive” PCa therapy, often preceding clinically detectable disease (26). Accurate delineation of local versus metastatic disease is imperative to determine appropriate therapy. Although MRI is widely used to assess local recurrence, its interpretation can be confounded by inherently low specificity and by the glandular atrophy and fibrosis induced by radiation. With respect to PET, PCa grows slowly, accounting for its lack of avidity for 18F-FDG, which has proved so successful for most other malignancies. Also, the bladder produces a strong ^{18}F-FDG signal near the prostate. The role of ^{11}C-choline, as previously described, is limited in detecting early recurrence by its inability to identify microscopic foci of metastatic PCa (27). Although higher urinary excretion of the fluorinated analogs represents a disadvantage in imaging PCa, 18F-fluorocholine PET/CT has demonstrated a sensitivity of 71% in localizing recurrent disease (28). ^{11}C-Acetate has also been evaluated for detection of recurrence and has demonstrated results comparable to those of ^{11}C-choline (29).

The prostate-specific membrane antigen (PSMA) is upregulated in PCa, particularly in advanced, hormone-independent, and metastatic disease. PSMA is an integral membrane protein with an enzymatic active site in an extracellular domain, making it an excellent target for imaging and therapy. The monoclonal antibody–based PSMA imaging agent, capromab pendetide, has demonstrated limited clinical utility. Other PSMA-binding antibodies such as J591, with an affinity to the extracellular domain of PSMA, are under development for imaging and may prove superior to capromab pendetide (30,31). Urea-based low-molecular-weight agents of high affinity and in vivo selectivity for PSMA have been synthesized using a variety of radionuclides for PET and SPECT (32–34). Compound $[^{99m}Tc(CO)_3(L1)]^+$ is one such example. Compounds of this class demonstrate high target-to-nontarget ratios and rapid washout from nontarget sites in both preclinical models (Fig. 2) and a phase 1 study (35). Initial indications for the use of these agents would be for staging and in patients who have undergone prostatectomy but later present with a rising PSA level.

There has been renewed interest in the use of ^{18}F-NaF-PET for early detection of metastases. A recent study has shown ^{18}F-NaF to be superior to bone scanning performed using the standard agent, ^{99m}Tcmethylene diphosphonate, with or without SPECT, in

detecting metastases (36). However, the ease of availability and lower cost render ^{99m}Tcmethylene diphosphonate more desirable for now.

ASSESSMENT OF RESPONSE TO THERAPY

1-(2′-Deoxy-2′-fluoro-β-D-arabinofuranosyl)thymidine (FMAU) is a thymidine analog phosphorylated by thymidine kinase and incorporated into DNA. 18F-FMAU has been evaluated for imaging PCa in 3 patients and showed a significantly elevated maximum standardized uptake value within the tumor, high uptake in bone metastases, and low uptake in a previously irradiated prostate bed. Only a small amount of radioactivity was demonstrated within the urinary bladder despite renal excretion (37). Like ^{18}F-FMAU, ^{18}F-fluorothymidine uptake is directly related to cell proliferation; however, no imaging of ^{18}F-fluorothymidine in patients with PCa has been published to date.

16β^{18}F-fluoro-5α-dihydrotestosterone (FDHT), an analog of 5a-dihydrotestosterone, has demonstrated a sensitivity of 86% for detection of metastatic and recurrent PCa (38). Patients with positive findings underwent a repeated examination after the administration of flutamide, an antiandrogen, and demonstrated an interval decrease in radiopharmaceutical uptake. That finding suggests that 18F-FDHT may be useful for evaluating the availability and functional status of tumor androgen receptor to monitor therapeutics that target it—a topic for future studies.

Molecular–genetic imaging provides a way to monitor gene therapy, especially to determine the level and volume of therapeutic gene expression, which can be correlated with clinical outcome. Barton et al. (39) recently conducted a phase 1 study demonstrating the feasibility of adenovirus-mediated gene therapy for PCa. Patients with clinically localized PCa were administered a replication-competent adenovirus, Ad5-yCD/*ut*TK$_{SR39}$*rep*-hNIS, armed with 2 suicide genes and the sodium iodide symporter (NIS) gene via an intraprostatic injection. NIS gene expression was imaged by uptake of ^{99m}Tc-$NaTcO_4$ in infected cells using SPECT, which showed a peak gene expression volume at 1–2 d after the adenovirus injection, detectable for up to 7 d. Whole-body SPECT demonstrated intraprostatic gene expression, without evidence of extraprostatic dissemination of the adenovirus, demonstrating the feasibility of this technology in humans.

Vasoactive intestinal peptide (VIP) and pituitary adenylate cyclase–activating peptide receptor (VPAC1) are overexpressed in 100% of human PCa (40). VIP$_{28,}$ a VIP analog radiolabeled with ^{64}Cu, specifically targets VPAC1 receptors for visualization of PCa by PET. ^{64}Cu, with a physical half-life of 12.7 h (β^+, 655 keV [17. 4%]; β^-, 573 keV [30%]), is commercially available, has well-known chemistry, provides quantitative yields, and permits the use of radiolabeled compounds without complex purification. ^{64}Cu-VIP$_{28}$ was tested in PCa xenografts in nude mice and in spontaneous PCa in TRAMP mice. The compound demonstrated a target-to-background ratio of 4.2 at 24 h after injection, suggesting its promise for future clinical studies.

PERSPECTIVE

Despite a variety of emerging techniques and probes using multiple imaging modalities, neither detection of minimal disease nor prediction of indolent versus aggressive PCa has been accomplished. A simple, accurate method for localizing cancer within the prostate for focal therapy also remains elusive. Although there are no definitive markers that can predict tumor progression for PCa, more careful study and validation of combinations of markers such as PSMA and androgen receptor may provide clues in approaching this pressing clinical issue. In addition to the continued search for molecular imaging agents with appropriate pharmacokinetics, key to addressing these important clinical problems will be

the merger of new, selective serum and urinary biomarkers, such as the urinary marker sarcosine, with molecular imaging tools. A practical multimodality imaging approach coupled with an array of relevant biomarkers sampled from the blood and urine will provide the best chance for effective if not tailored management of PCa.

Acknowledgments

We acknowledge the National Institutes of Health (grants CA92871 and CA134675) and the Prostate Cancer Foundation for support.

REFERENCES

1. Jemal A, Siegel R, Ward E, et al. Cancer statistics, 2008. CA Cancer J Clin. 2008; 58:71–96. [PubMed: 18287387]
2. Schroder FH, Hugosson J, Roobol MJ, et al. Screening and prostate-cancer mortality in a randomized European study. N Engl J Med. 2009; 360:1320–1328. [PubMed: 19297566]
3. Sreekumar A, Poisson LM, Rajendiran TM, et al. Metabolomic profiles delineate potential role for sarcosine in prostate cancer progression. Nature. 2009; 457:910–914. [PubMed: 19212411]
4. Kelloff GJ. Issues in clinical prostate cancer: role of imaging. AJR. 2009; 192:1455–1470. [PubMed: 19457806]
5. Bak JB, Landas SK, Haas GP. Characterization of prostate cancer missed by sextant biopsy. Clin Prostate Cancer. 2003; 2:115–118. [PubMed: 15040873]
6. Futterer JJ, Engelbrecht MR, Jager GJ, et al. Prostate cancer: comparison of local staging accuracy of pelvic phased-array coil alone versus integrated endorectal-pelvic phased-array coils—local staging accuracy of prostate cancer using endorectal coil MR imaging. Eur Radiol. 2007; 17:1055–1065. [PubMed: 17024497]
7. Mueller-Lisse UG, Scherr MK. Proton MR spectroscopy of the prostate. Eur J Radiol. 2007; 63:351–360. [PubMed: 17709223]
8. Wefer AE, Hricak H, Vigneron DB, et al. Sextant localization of prostate cancer: comparison of sextant biopsy, magnetic resonance imaging and magnetic resonance spectroscopic imaging with step section histology. J Urol. 2000; 164:400–404. [PubMed: 10893595]
9. Costouros NG, Coakley FV, Westphalen AC, et al. Diagnosis of prostate cancer in patients with an elevated prostate-specific antigen level: role of endorectal MRI and MR spectroscopic imaging. AJR. 2007; 188:812–816. [PubMed: 17312072]
10. Zakian KL, Sircar K, Hricak H, et al. Correlation of proton MR spectroscopic imaging with Gleason score based on step-section pathologic analysis after radical prostatectomy. Radiology. 2005; 234:804–814. [PubMed: 15734935]
11. Klomp DW, Bitz AK, Heerschap A, Scheenen TW. Proton spectroscopic imaging of the human prostate at 7 T. NMR Biomed. 2009; 22:495–501. [PubMed: 19170072]
12. Singh AK, Kruecker J, Xu S, et al. Initial clinical experience with real-time transrectal ultrasonography-magnetic resonance imaging fusion-guided prostate biopsy. BJU Int. 2008; 101:841–845. [PubMed: 18070196]
13. Bax J, Cool D, Gardi L, et al. Mechanically assisted 3D ultrasound guided prostate biopsy system. Med Phys. 2008; 35:5397–5410. [PubMed: 19175099]
14. Albers MJ, Bok R, Chen AP, et al. Hyperpolarized 13C lactate, pyruvate, and alanine: noninvasive biomarkers for prostate cancer detection and grading. Cancer Res. 2008; 68:8607–8615. [PubMed: 18922937]
15. Testa C, Schiavina R, Lodi R, et al. Prostate cancer: sextant localization with MR imaging, MR spectroscopy, and 11C-choline PET/CT. Radiology. 2007; 244:797–806. [PubMed: 17652190]
16. Giovacchini G, Picchio M, Coradeschi E, et al. [^{11}C]choline uptake with PET/CT for the initial diagnosis of prostate cancer: relation to PSA levels, tumour stage and anti-androgenic therapy. Eur J Nucl Med Mol Imaging. 2008; 35:1065–1073. [PubMed: 18200444]

17. Kwee SA, Thibault GP, Stack RS, Coel MN, Furusato B, Sesterhenn IA. Use of step-section histopathology to evaluate 18F-fluorocholine PET sextant localization of prostate cancer. Mol Imaging. 2008; 7:12–20. [PubMed: 18384719]
18. Oyama N, Akino H, Kanamaru H, et al. 11C-acetate PET imaging of prostate cancer. J Nucl Med. 2002; 43:181–186. [PubMed: 11850482]
19. Schuster DM, Votaw JR, Nieh PT, et al. Initial experience with the radiotracer anti-1-amino-3-18F-fluorocyclobutane-1-carboxylic acid with PET/CT in prostate carcinoma. J Nucl Med. 2007; 48:56–63. [PubMed: 17204699]
20. Bloch BN, Furman-Haran E, Helbich TH, et al. Prostate cancer: accurate determination of extracapsular extension with high-spatial-resolution dynamic contrast-enhanced and T2-weighted MR imaging: initial results. Radiology. 2007; 245:176–185. [PubMed: 17717328]
21. Harisinghani MG, Barentsz J, Hahn PF, et al. Noninvasive detection of clinically occult lymph-node metastases in prostate cancer. N Engl J Med. 2003; 348:2491–2499. [PubMed: 12815134]
22. van As NJ, de Souza NM, Riches SF, et al. A study of diffusion-weighted magnetic resonance imaging in men with untreated localised prostate cancer on active surveillance. Eur Urol. Dec 6.2008 Epub ahead of print.
23. Kurhanewicz J, Vigneron D, Carroll P, Coakley F. Multiparametric magnetic resonance imaging in prostate cancer: present and future. Curr Opin Urol. 2008; 18:71–77. [PubMed: 18090494]
24. Tamada T, Sone T, Jo Y, et al. Apparent diffusion coefficient values in peripheral and transition zones of the prostate: comparison between normal and malignant prostatic tissues and correlation with histologic grade. J Magn Reson Imaging. 2008; 28:720–726. [PubMed: 18777532]
25. Xu J, Humphrey PA, Kibel AS, et al. Magnetic resonance diffusion characteristics of histologically defined prostate cancer in humans. Magn Reson Med. 2009; 61:842–850. [PubMed: 19215051]
26. Partin AW, Pound CR, Clemens JQ, Epstein JI, Walsh PC. Serum PSA after anatomic radical prostatectomy: the Johns Hopkins experience after 10 years. Urol Clin North Am. 1993; 20:713–725. [PubMed: 7505980]
27. Scattoni V, Picchio M, Suardi N, et al. Detection of lymph-node metastases with integrated [11C]choline PET/CT in patients with PSA failure after radical retropubic prostatectomy: results confirmed by open pelvic-retroperitoneal lymphadenectomy. Eur Urol. 2007; 52:423–429. [PubMed: 17397992]
28. Husarik DB, Miralbell R, Dubs M, et al. Evaluation of [18F]-choline PET/CT for staging and restaging of prostate cancer. Eur J Nucl Med Mol Imaging. 2008; 35:253–263. [PubMed: 17926036]
29. Morris MJ, Scher HI. 11C-acetate PET imaging in prostate cancer. Eur J Nucl Med Mol Imaging. 2007; 34:181–184. [PubMed: 17238014]
30. Nargund V, Al Hashmi D, Kumar P, et al. Imaging with radiolabelled monoclonal antibody (MUJ591) to prostate-specific membrane antigen in staging of clinically localized prostatic carcinoma: comparison with clinical, surgical and histological staging. BJU Int. 2005; 95:1232–1236. [PubMed: 15892807]
31. Elsasser-Beile U, Reischl G, Wiehr S, et al. PET imaging of prostate cancer xenografts with a highly specific antibody against the prostate-specific membrane antigen. J Nucl Med. 2009; 50:606–611. [PubMed: 19289418]
32. Mease RC, Dusich CL, Foss CA, et al. N-[N-[(S)-1,3-dicarboxypropyl]carbamoyl]-4-[18F]fluorobenzyl-L-cysteine, [18F]DCFBC: a new imaging probe for prostate cancer. Clin Cancer Res. 2008; 14:3036–3043. [PubMed: 18483369]
33. Banerjee SR, Foss CA, Castanares M, et al. Synthesis and evaluation of technetium-99m- and rhenium-labeled inhibitors of the prostate-specific membrane antigen (PSMA). J Med Chem. 2008; 51:4504–4517. [PubMed: 18637669]
34. Kularatne SA, Zhou Z, Yang J, Post CB, Low PS. Design, synthesis, and preclinical evaluation of prostate-specific membrane antigen targeted ^{99m}Tc-radioimaging agents. Mol Pharm. 2009; 6:790–800. [PubMed: 19361232]
35. Barrett JA, LaFrance N, Coleman RE, et al. Targeting metastatic prostate cancer [PCa] in patients with 123I-MIP1072 and 123I-MIP1095 [abstract]. J Nucl Med. 2009; 50(suppl):136P.

36. Even-Sapir E, Metser U, Mishani E, Lievshitz G, Lerman H, Leibovitch I. The detection of bone metastases in patients with high-risk prostate cancer: ^{99m}Tc-MDP planar bone scintigraphy, single- and multi-field-of-view SPECT, 18F-fluoride PET, and 18F-fluoride PET/CT. J Nucl Med. 2006; 47:287–297. [PubMed: 16455635]

37. Sun H, Sloan A, Mangner TJ, et al. Imaging DNA synthesis with [18F]FMAU and positron emission tomography in patients with cancer. Eur J Nucl Med Mol Imaging. 2005; 32:15–22. [PubMed: 15586282]

38. Dehdashti F, Picus J, Michalski JM, et al. Positron tomographic assessment of androgen receptors in prostatic carcinoma. Eur J Nucl Med Mol Imaging. 2005; 32:344–350. [PubMed: 15726353]

39. Barton KN, Stricker H, Brown SL, et al. Phase I study of noninvasive imaging of adenovirus-mediated gene expression in the human prostate. Mol Ther. 2008; 16:1761–1769. [PubMed: 18714306]

40. Zhang K, Aruva MR, Shanthly N, et al. PET imaging of VPAC1 expression in experimental and spontaneous prostate cancer. J Nucl Med. 2008; 49:112–121. [PubMed: 18077536]

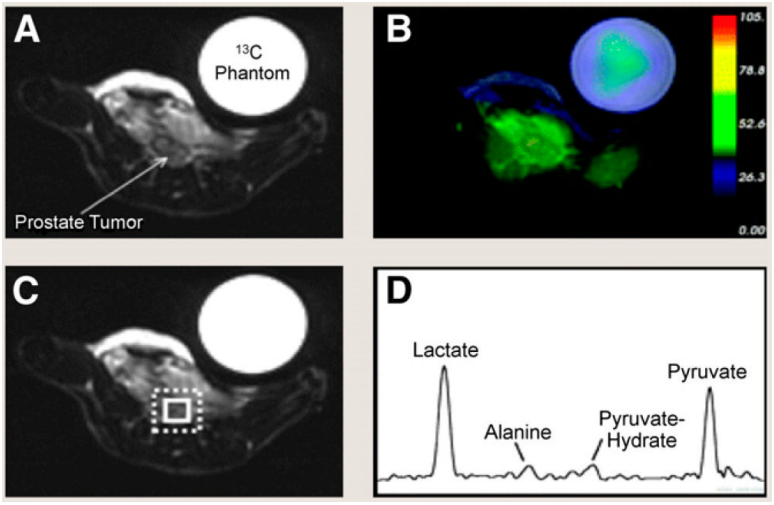

FIGURE 1.

Detection of low-grade PCa with MRS using hyperpolarized ^{13}C-labeled pyruvate. T2-weighted ^{1}H image depicting low-grade primary tumor in TRAMP mouse (A), overlay of interpolated hyperpolarized ^{13}C lactate image (B), and spectral grid (C and D). Spectrum shows prominent signals from lactate and pyruvate and smaller signals from alanine and pyruvate hydrate. (Adapted with permission of (14).)

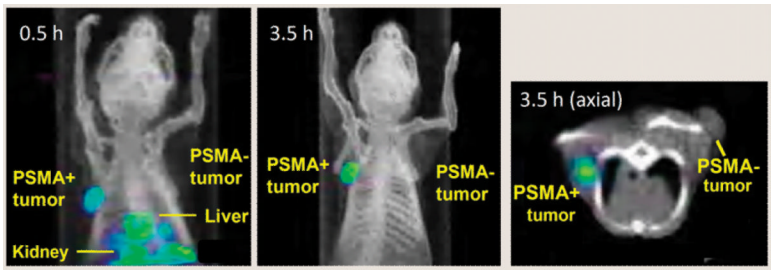

FIGURE 2.

Imaging PCa using urea-based low-molecular-weight agents. Dual-pinhole SPECT/CT of PC-3 PIP (PSMA+) and PC-3 flu (PSMA2–) tumor-bearing mouse with $[^{99m}Tc(CO)_3(L1)]^+$. Note lack of radiopharmaceutical out-side of the tumor. (Adapted with per-mission of (33).)